

## 1 Supplementary Material to

### 2 “Smooth Muscle Contractility Causes the Gut to Grow Anisotropically”

3 Diana Khalipina, Yusuke Kaga, Nicolas Dacher, Nicolas R. Chevalier

4 Laboratoire Matière et Systèmes Complexes, Université Paris Diderot/CNRS UMR 7057, Sorbonne  
5 Paris Cité, 10 rue Alice Domon et Léonie Duquet, 75013 Paris, France

6 \* Corresponding author : [nicolas.chevalier@univ-paris-diderot.fr](mailto:nicolas.chevalier@univ-paris-diderot.fr)

7 Journal of the Royal Society Interface - 2019

8

#### 9 **Characterization of passive mechanical properties**

10 Tensile testing and pressurization tests were performed as previously described (38). Briefly, for  
11 tensile testing, the hindgut was pinned to the bottom of a Sylgard coated trough filled with ~100 mL  
12 DPBS (0.9 mM Ca<sup>2+</sup>, 0.49 mM Mg<sup>2+</sup>). The stomach of the guts was attached to a hook formed at the  
13 end of a thin glass cantilever (Figure 2a). The sensitivity (force per deflection angle) of the cantilever  
14 was determined by calibration with weights prior to the experiment. The cantilever was pulled at a  
15 constant velocity of 0.3 mm/sec to stretch the guts. The deformation of the gut tract and the deflection  
16 of the pipette were monitored with a camera and measured with ImageJ. Each gut was stretched three  
17 times, waiting 20 minutes between each stretch to ensure that the gut relaxed back to its initial length.  
18 For inflation experiments, ~1 cm long midgut segments were cannulated with a thin glass pipette; we  
19 tightened knots made out of hair at the gut-pipette junction and at the free end of the gut to allow  
20 pressure build-up inside the gut. Pressure was applied with a syringe filled with DPBS. We monitored  
21 the change in length, diameter and thickness of the gut wall; the latter could be discerned from luminal  
22 content by coloring the injected solution with a dye (methylene blue).

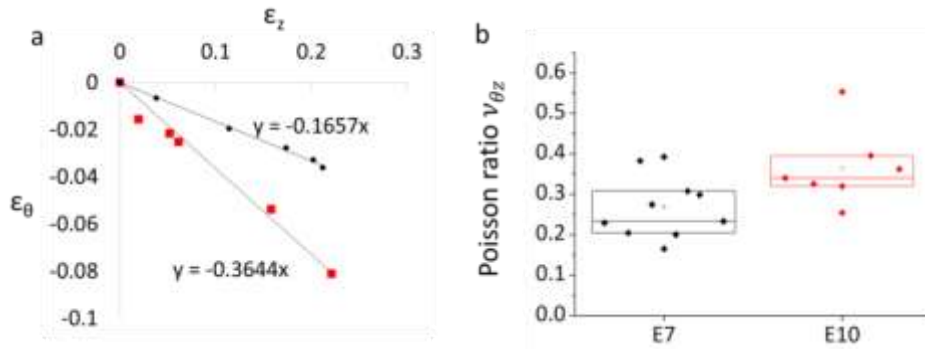
#### 23 **Computation of elastic moduli**

24 We computed the longitudinal elastic modulus  $E_z$  from the slope of the stress-strain data (Fig.2b),  
25 where the longitudinal stress is  $\sigma_z = f/S$  with  $f = s\Delta\alpha$  the force applied by the cantilever,  $s$  the  
26 sensitivity (mN/°) of the cantilever,  $\Delta\alpha$  its deflection angle and  $S$  the section of the gut. For E7 guts  
27 the lumen cross-section is negligible so that  $S = \pi d^2/4$ , with  $d$  the average diameter of the gut  
28 segment. For E10 guts, the lumen occupies ~5% of the gut cross-section(7) so that  $S = 0.95 \pi d^2/4$ .

29 During phase II and III (Fig.2e) of pressurization, the gut wall thickness changes little (II) or not at all  
30 (III). In this configuration, the gut can be considered as an orthotropic, thin-walled cylinder with  
31 anisotropic mechanical properties along two directions (longitudinal and orthoradial). The governing  
32 equations are  $\varepsilon_z = \frac{\sigma_z}{E_z} - \frac{\nu_{\theta z}}{E_\theta} \cdot \sigma_\theta$  (1) and  $\varepsilon_\theta = -\frac{\nu_{z\theta}}{E_z} \cdot \sigma_z + \frac{\sigma_\theta}{E_\theta}$  (2), where  $\varepsilon_z$  and  $\varepsilon_\theta$  are the strains,  $E_z$   
33 and  $E_\theta$  the elastic moduli and  $\sigma_z$  and  $\sigma_\theta$  the stresses along the longitudinal and orthoradial directions  
34 respectively;  $\nu_{\theta z}$  and  $\nu_{z\theta}$  are the associated Poisson coefficient and are related by  $\nu_{z\theta} = \frac{E_z}{E_\theta} \nu_{\theta z}$  for an  
35 orthotropic material. The strains  $\varepsilon_z = (z - z_0)/z_0$  and  $\varepsilon_\theta = (d - d_0)/d_0$  were obtained from high-  
36 magnification videos of the guts during the inflation, where  $z$  and  $d$  are the length and exterior  
37 diameter of the gut segment when a pressure  $p$  is applied, and  $z_0$  and  $d_0$  are the initial length and  
38 diameter at the start of phase II (or phase III) of the inflation. For a thin-walled cylinder, the  
39 orthoradial (hoop stress) and longitudinal stress are related to the pressure(41) by  $\sigma_\theta = \frac{pr}{h}$  (3) and  
40  $\sigma_z = \frac{pr}{2h}$  (4). Combining (1-4), we find  $E_\theta = 2E_z \left[ \frac{\varepsilon_z}{\varepsilon_\theta} \left( 1 - \frac{\nu_{\theta z}}{2} \right) + \nu_{\theta z} \right] \cdot \frac{\varepsilon_z}{\varepsilon_\theta}$  was measured for each  
41 inflation from linear fits of  $\varepsilon_z$  vs  $\varepsilon_\theta$  data (Fig.2f). The Poisson modulus of the guts  $\nu_{\theta z} = \varepsilon_\theta/\varepsilon_z$  was  
42 obtained by measuring the decrease in diameter  $\varepsilon_\theta$  when an applied, constant longitudinal strain  $\varepsilon_z$   
43 was applied (Fig.S1). We found  $\nu_{\theta z,E7} = 0.27 \pm 0.08$  ( $n=10$ ) and  $\nu_{\theta z,E10} = 0.36 \pm 0.09$  ( $n=7$ ).

#### 44 **Second Harmonic Generation Microscopy**

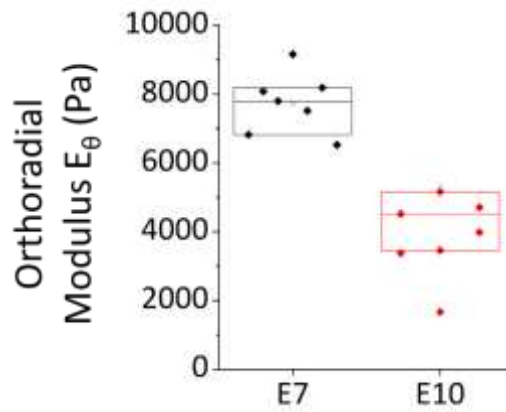
45 We used a vibratome to cut 150  $\mu\text{m}$ -thick transverse sections of E9 jejunum embedded in 3% agarose  
46 type VII (Sigma); longitudinal sections from the same sample were then collected. Image acquisition  
47 was performed in the IMAG'IC Facility, Institut Cochin, Paris, France. SHG images were obtained  
48 with an upright Leica SP5 microscope (Leica Microsystems GmbH, Wetzlar, Germany) coupled to a  
49 femtosecond Ti:sapphire laser (Chameleon, Coherent, Saclay, France) tuned to a wavelength of 810  
50 nm for all experiments. The beam was circularly polarized. We used a Leica Microsystems HCX  
51 IRAPO 25x/0.95 W objective. The SHG signal was detected in epi-collection through a 405/15-nm  
52 bandpass filter, by an NDD PMT (Leica Microsystems), with a fixed voltage supply, laser excitation  
53 power and exposure time, allowing the direct comparison of SHG signal intensities on transverse and  
54 longitudinal sections. Z-stacks of each sample were collected (total  $z = 120 \mu\text{m}$ , step  $\Delta z = 3 \mu\text{m}$ ) and the  
55 maximum values of the stacks were projected. Collagen fibers contribute ~50% (15) to passive tissue  
56 mechanical properties.



57

58 Figure S1: Poisson ratio of E7 and E10 midgut. (a) Example of diameter change  $\epsilon_\theta$  as a longitudinal strain  $\epsilon_z$  is  
 59 applied, at E7 (black) and E10 (red). (b) Measured Poisson modulus  $\nu_{\theta z} = \epsilon_\theta / \epsilon_z$  at E7 ( $n=10$ ) and E10 ( $n=7$ ).

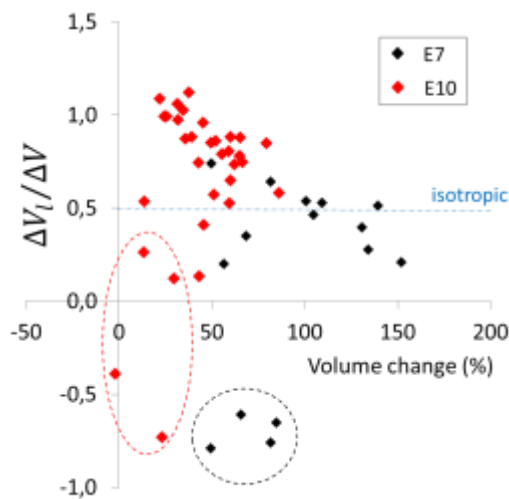
60



61

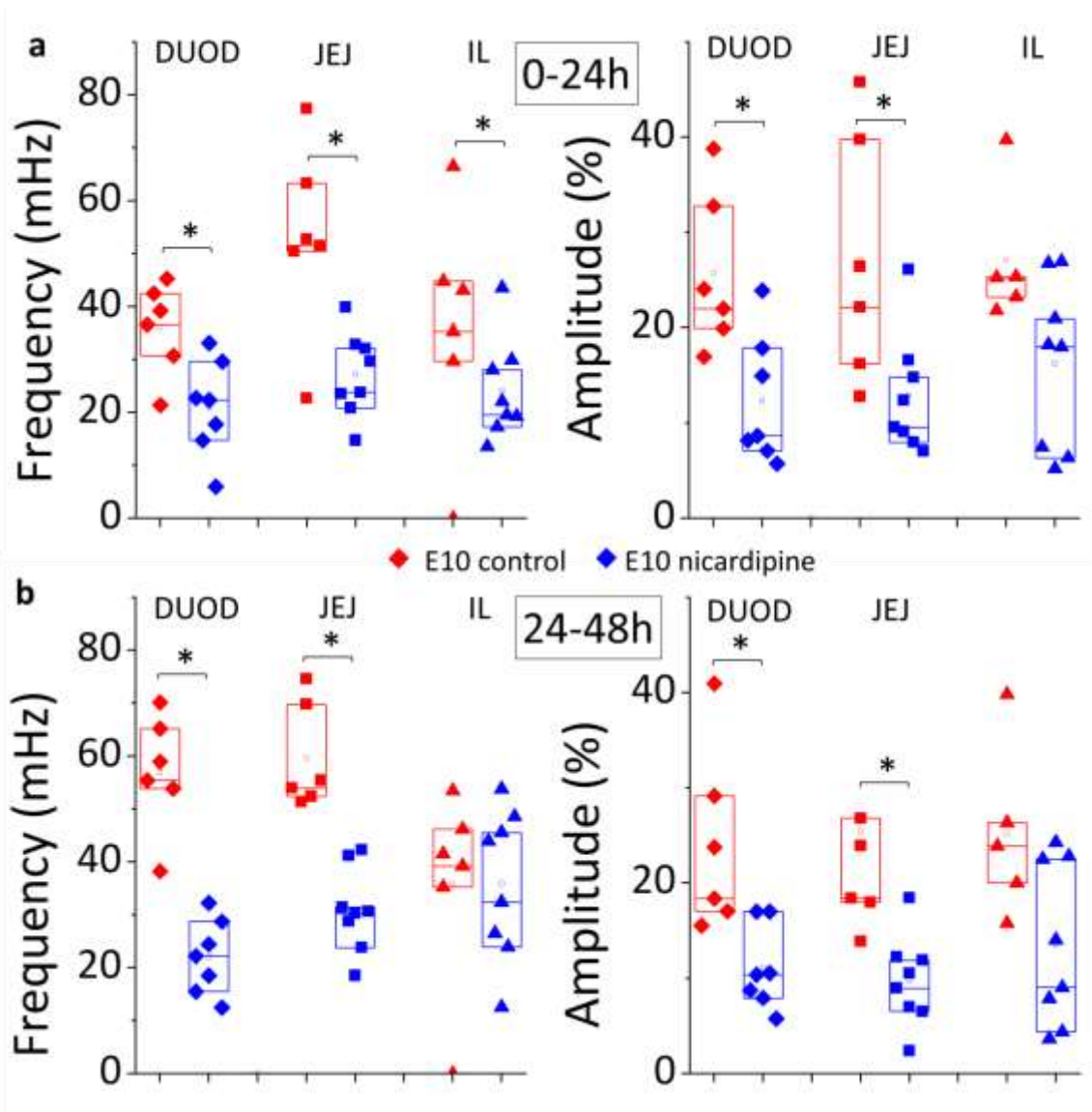
62 Figure S2. Orthoradial elastic modulus  $E_\theta$  at E7 ( $n=7$ ) and E10 ( $n=9$ ), derived from phase III of pressurization.

63



64

65 Figure S3. Relative lengthening  $\Delta V_l / \Delta V$  after 2 day culture as a function of the observed volume change, for E7 and  
 66 E10 guts. Outliers in each age group (dashed ovals) exhibit a small volume change, in the lower half of the average  
 67 volume change of each age group. This indicates that the unusual behavior of these samples may arise from poor  
 68 vitality of the organ following dissection or during culture.

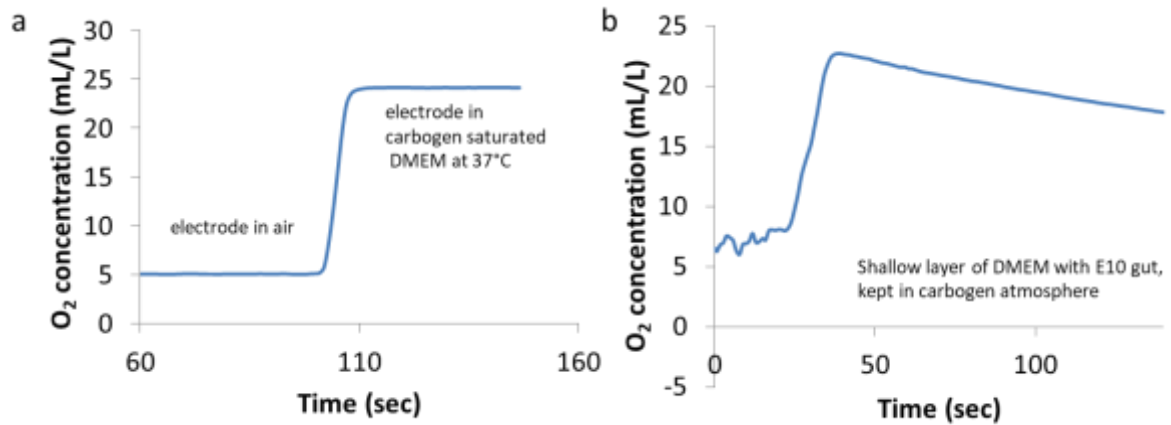


70

71 Figure S4. Nicardipine 5  $\mu\text{M}$  reduces the amplitude and frequency of spontaneous contractions during 48 h culture.  
 72 (a,b) Frequency and amplitude of contractions of control (red) and nicardipine (5  $\mu\text{M}$ ) treated guts (blue) during the  
 73 first (a) and the second (b) day of culture. Each data point is a different gut, and is the mean of data sampled at 2, 8  
 74 and 22 h after application (or renewal at 24 h) of the medium with vehicle or drug. DUOD: duodenum, JEJ: jejunum,  
 75 IL: ileum. \* $p < 0.05$ , Mann Whitney two-tailed test.

76

77



78

79 **Figure S5.** Clark-type electrode measurements of O<sub>2</sub> in (a) 40 mL DMEM at 37°C bubbled with carbogen, used for  
 80 gut growth in Fig.3. (b) Shallow layer of DMEM (1 mL in 35 mm Petri dish) with E10 gut sample as used in Fig.4,  
 81 after 4h culture. The electrode was quickly inserted in the medium, ~1 cm away from the gut. The oxygen  
 82 concentration relaxes to lower values because the measurement is performed in air and the sample gradually  
 83 equilibrates with atmospheric O<sub>2</sub>. The maximum of the curve was measured.

84

85

86

## 87 **Supplementary Videos**

88 VideoS1: Compared peristaltic activity of E7 and E10 guts.

89 Video S2: Effect of calcium channel blocker CoCl<sub>2</sub> on E7 and E10 gut morphology and peristaltic  
 90 activity.

91 Video S3: Pressurization of E7 and E10 guts.

92 VideoS4: Peristalsis of E10 guts in culture system with injected O<sub>2</sub>, after 48h culture.

93 VideoS5: Time-lapse of E10 guts elongating in culture system with injected O<sub>2</sub>, first 6 hours of  
 94 culture.

95

96